Comparative Medicine
Copyright 2008
by the American Association for Laboratory Animal Science

Vol 58, No 2
April 2008
Pages 174–179

Porcine Models in Spinal Research: Calibration and Comparative Finite Element Analysis of Various Configurations during Flexion–Extension

Hadi N Aziz,[1,*] Fabio Galbusera,[1] Chiara Maria Bellini,[1] Giuseppe Vincenzo Mineo,[1,2] Alessandro Addis,[3] Riccardo Pietrabissa,[4] and Marco Brayda-Bruno[1]

This study was conducted to develop and calibrate a detailed 3-dimensional finite element model of the porcine lumbar spine and to compare this model with various configurations in flexion and extension. Computed tomography scans obtained from the L4–L5 lumbar segment of a Landrace × Large White pig were used to generate a solid volume. The various passive components were characterized by using a step-by-step calibration procedure in which the material properties of the anatomic structures were modified to match the corresponding in vitro data set-points retrieved from the literature. The range of motion of the totally assembled intact model was assessed under a 10-Nm flexion–extension moment and compared with data from a bilateral complete and hemifacetectomy configuration. In addition, the results from our porcine model were compared with published data regarding range of motion in a human finite element model in order to predict the configuration of the porcine model that most closely represented the human spine. Both the intact and hemifacetectomy configurations of the porcine model were comparable to the human spine. However, qualitative analysis of the instantaneous axis of rotation revealed a dissimilarity between the intact porcine model and human spine behavior, indicating the hemifacetectomy configuration of the porcine model as the most appropriate for spinal instrumentation studies. The present 3-dimensional finite element porcine model offers an additional tool to improve understanding of the biomechanics of the porcine spine and to decrease the expense of spinal research.

Abbreviations: CL, capsular ligament, FE, finite element; FJ, facet joint; IAR, instantaneous axes of rotation; ISL, interspinous ligament; IVD, intervertebral disc; LF, ligamentum flavum; RoM, range of motion; SSL, supraspinous ligament

Animal models have played a vital role in numerous medical advances in spinal research. Although important considerations concerning quadrupedal models have arisen, particularly regarding the fact that the loads applied to the ambulating porcine spine are quite different from those applied on the ambulating human spine, porcine specimens have been used successfully as models for biomechanical testing of human spine instrumentation techniques, spinal instability, and spinal fusion.[3] Indeed, several ex vivo animal models, including canine,[19] ovine,[24] cetaceous,[16] and bovine[2,5] have traditionally been used to evaluate the passive components of spinal stability. In addition, the geometric parameters of the intervertebral disc (IVD) from several animal species have been measured for comparisons with human lumbar disc geometry.[18] That study concluded that the mouse and rat lumbar and mouse tail discs offer the closest representations of the human lumbar IVD geometry.

However, despite differences in facet orientation and contour, the relative similarities in size and geometry of the vertebral anatomy were sufficient to warrant widespread use of porcine lumbar spinal models. In fact, the anatomic features of the L4 lumbar vertebra of the commonly available species used for large animal spine research have been characterized;[17] these data indicate that vertebrae from healthy farm-bred pigs most closely modeled human specimens in terms of transverse process length, interfacet distance, pedicle angle, vertebral body depth, and pedicle diameter and shape. However, facet contour is important in choosing the model best suited for studies of instabilities.[17]

Several ex vivo experiments have been conducted to determine the dependence of the mechanical properties of each of the passive components on the porcine lumbar spine. The mechanical behavior of the IVD and its dependence on the vertebral level was evaluated through compressive and shear tests on 3 adjacent minipig lumbar discs,[6] whereas stress distribution in porcine IVD was tested by using adult porcine cadaver lumbar functional spine units.[22] Experiments on standard farm pigs have addressed the biomechanical role of the lumbar spinal ligaments in flexion and extension:[11] the contribution of each ligament was determined by using a parallel-linkage robot. In other studies, these same investigators characterized the flexion–extension moment-angle properties of porcine lumbar segments by using sixth-order polynomials[7] and recommended the use of multisegmental specimens when performing flexion studies to appropriately represent the anatomic boundary conditions.[8] Porcine models also have been used to illustrate the structural and mechanical properties of the longitudinal ligaments and ligamentum flavum of the spine.[14]

Ex vivo experiments provide the most direct and obvious way to obtain information on spinal biomechanics and performance,

Received: 20 July 2007. Revision requested: 21 Aug 2007. Accepted: 12 Oct 2007.
[1]IRCCS Galeazzi Orthopaedic Institute, Milan, Italy; [2]Orthopaedic Clinics, [3]Veterinary Medicine Faculty, Università degli Studi di Milano, Milan, Italy; [4]Department of Structural Engineering, Politecnico Di Milano, Milan, Italy
[*]Corresponding author. Email: hadi.aziz@grupposandonato.it

but they can be expensive and unwieldy and suffer from interspecimen variability and issues of repeatability, although that variability itself will be an important parameter in the spine's characteristics. A finite element (FE) model of the porcine lumbar spine has not yet been reported in the literature. Computational modeling has the advantage that numerous and diverse specimens can be generated and examined. In addition, the same computational model can be used for any number of loading conditions and configurations, and the model itself can be modified to reproduce any physiologic condition. Further, computational modeling can provide a wealth of information that ex vivo experimentation cannot, such as stress distribution through the discs and vertebral bodies.

The purpose of the present study was to create and calibrate A FE model of porcine lumbar spine motion segment (L4-L5), identifying the appropriate material properties for its passive components. The importance of such a model is that it is an effective alternative to cadaver specimens, thereby increasing the cost-effectiveness of the associated research. In addition, because of the dependence of the ex vivo model on the facet contour[17] and in light of the lack of published data regarding porcine FE models, we also analyzed various configurations of the FE model to identify the one that most closely represents the human spine.

Materials and Methods

FE model set-up. A 3-dimensional reconstruction of the solid volume based on planar computer tomography images was set up by using appropriate commercial segmentation and visualization software (Amira, TGS, San Diego, CA). These images were taken from the lumbar spine of a healthy farm-bred (Landrace × Large White) pig weighing 60 kg and processed in a local abattoir for the food industry.[11] The segment chosen included 2 vertebrae (L4 to L5) from the 6 units present in the intact porcine lumbar spine. The solid model then was exported into a readable input file for FE preprocessor software (Gambit, Ansys Inc., Canonsburg, PA, USA), where the intervertebral disc was shaped. The bony components and IVD then were meshed (Figure 1) by using linear tetrahedral elements.

Because of the lack of reliable published data regarding the mechanical properties of both the porcine annulus fibrosus and nucleus pulposus, a nonlinear stress–strain curve for the entire IVD of the spinal segment[6] was implemented into the mathematical model through an appropriate calibration method. The IVD was modeled as an almost-incompressible unique material having a Poisson ratio of 0.49.

The vertebral bodies were modeled as cancellous continuum core surrounded by cortical shell. The shell thickness was assumed to be 0.45 mm[1,13] for both the lateral areas and endplates. Data regarding mechanical parameters of cancellous and cortical bone of the porcine vertebral body were achieved from already existing studies.[15,21] Because of the lack published data, the posterior bone was modeled as for human models[4,10] as a linear elastic orthotropic material, thus providing greater stiffness in the axial direction.

Bundles of nonlinear springs were used to represent the ligamenta flava (LF) and the capsular (CL), interspinous (ISL), and supraspinous (SSL) ligaments. Each of these ligaments was defined as 1 or more springs connecting the appropriate insertion points, and nonlinear load-displacement behaviors were adopted. The resistance to flexion and extension, offered by the anterior and posterior longitudinal ligaments, were included into the IVD behavior during the calibration procedure.

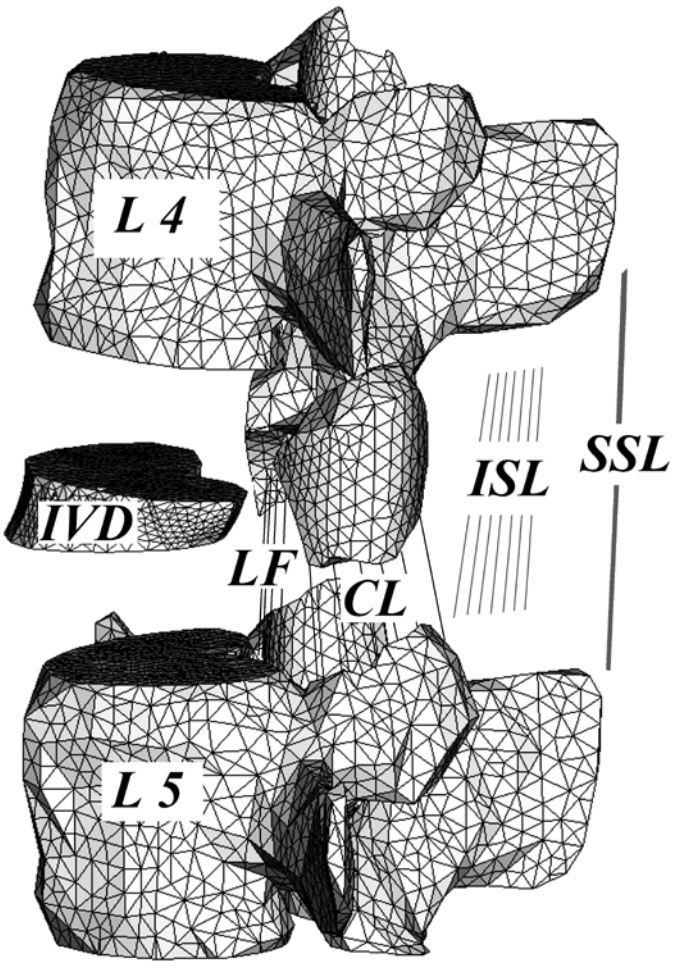

Figure 1. Exploded drawing of the L4–L5 FE-model of the porcine lumbar segment. IVD, intervertebral disc; SSL, supraspinous ligament; ISL, interspinous ligament; LF, ligamentum flavum; CL, capsular ligament.

The contact between articular facets of the posterior processes was simulated by surface-to-surface contact elements without friction.

Calibration procedure. To perform the FE-model calibration process, in vitro range of motion (RoM) data were achieved from a previously reported study[11] in which a pure moment load was applied to 11 spinal specimens from farm-bred crossbred pigs weighing 55 to 65 kg by using a parallel-linkage robot. Each specimen was tested 6 times, with sequential resections in the following sequence: intact; removal of the interaction between the SSL and the ISL; removal of the SSL; removal of the ISL; removal of the LF; and finally removal of the facet joint complexes (FJ) through complete facetectomy. The anterior and the posterior longitudinal ligaments were left intact throughout the experiment. The kinematic pathway was repeated for each of these tests and, accordingly, the changes in loads between trials reflected the mechanics of the removed structures.

To complement the experimental study just described, the caudal endplate of the L5 vertebral body was rigidly fixed, anchoring the relative elements, while a pure sagittal moment was applied to the cranial end of L4 vertebral body in order to simulate pure

flexion and extension motion. The present FE model then was calibrated stepwise, starting with the complete facetectomy condition (No-FJ condition) and followed respectively by insertion of each of the anatomical components removed in the earlier study, including the FJ (No-LF condition), LF (No-ISL condition), ISL (No-SSL condition), and SSL (intact condition). Each addition of an anatomic component required a new calibration, so that the material properties of the added anatomic structures were modified to match the corresponding in vitro data set-point.

Although the in vitro experiments were controlled to obtain similar motion between tests and to obtain the decrease in peak moment as the dependent variable,[11] the computational simulations in this study were conducted under a load-control approach, in which the peak flexion–extension moments were assumed to be similar to those achieved from the moment–angle curves of the experimental study. Accordingly, the No-FJ condition was tested under a 7-Nm peak extension moment, whereas a 14-Nm pure extension moment was applied to the remaining 4 conditions. In contrast, a different peak flexion moment was applied to each of the 5 conditions. The different conditions and the relative peak flexion–extension moments applied are summarized in Table 1.

For each bending moment, the corresponding IVD stress-strain curve or ligament stiffness was calibrated adequately. A starting curve was assumed initially by using a set of data points that were optimized to match the in vitro data; these subsequently were interconnected by using a spline function describing a continuous curve.

Comparison of FE models. Once the mechanical behavior of the intact condition had been determined, 4 configurations were compared under a pure 10-Nm flexion–extension moment (Table 1). An intact porcine lumbar segment was tested, and resulting RoM values were compared with those of hemifacetectomy and complete facetectomy configurations of the porcine model and a human computational lumbar model (L4–L5) retrieved from the literature.[20] The hemifacetectomy configuration was obtained by splitting of the posterior closing part of the FJ contour through an adequate hemifacetectomy cut plane as shown in Figure 2 and reducing the relative contribution of the capsular ligament. The hemifacetectomy cut-plane was oriented in order to subdivide the surface area of the FJ into 2 equal parts.

In addition to the RoM results, we qualitatively compared the locations of the instantaneous axes of rotation (IAR). The comparison assessed the areas containing the positions of individual IARs for each 1° of extension motion for the intact, hemifacetectomy, and complete facetectomy porcine configurations.

Table 1. Schematic step-by-step representation of the conditions applied during the calibration procedure, with the relative peak flexion–extension moment assumed for the numeric simulations conducted on the present FE model (upper). Schematic representation of the different configurations of the porcine segment compared in this study, under a 10 Nm flexion-extension moment (lower). Data for the intact human configuration were retrieved from the literature.[20]

STEP_BY STEP CALIBRATION	Peak flexion Moment (Nm)	Peak extension Moment (Nm)
No-FJ condition	4	7
No-LF condition	6	14
No-ISL condition	10	14
No-SSL condition	12	14
Intact condition	16	14
FE CONFIGURATIONS		
Intact porcine	10	10
Hemi-facetectomy	10	10
Facetectomy	10	10
Intact Human (21)	10	10

SSL, supraspinous ligament; ISL, interspinous ligament; LF, ligamentum flavum; CL, capsular ligament.

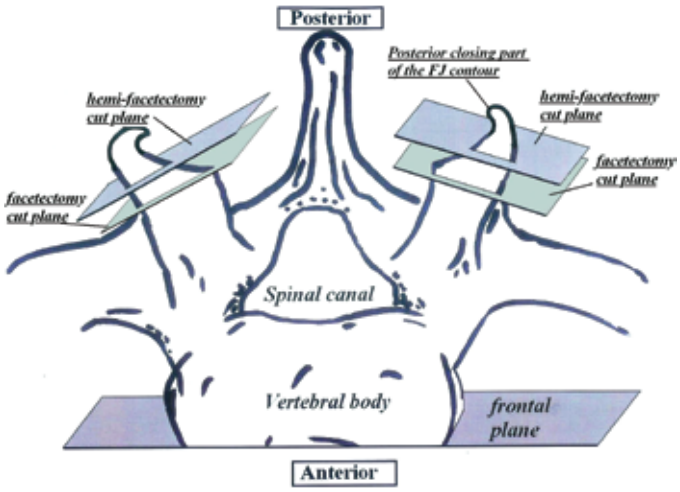

Figure 2. Cranial to caudal drawing view of a porcine vertebra. Both the facetectomy and hemifacetectomy cut planes are shown, and the posterior closing contribution of the facet joint complex is illustrated.

Results

FE analysis was used TO evaluate the passive spinal element properties of a porcine lumbar segment. Figure 3 shows the nonlinear stress–strain calibrated curve of the L4–L5 IVD. For each step of calibration, the FE model was in excellent agreement with in vitro RoM data (Table 2).

Force–displacement nonlinear curves for the CL, SSL, ISL, and LF of the calibrated FE model in comparison with the relative ligaments of a human FE model[20] are shown in Figure 4. The force-displacement curves of the CL and SSL were similar to those of their relative human ligaments, with both porcine ligaments showing increased stiffness. In contrast, the porcine ISL and LF demonstrated an inverse contribution with respect to their human counterparts: the porcine ISL behaved like the human LF, and the porcine LF behaved like the human ISL. The porcine ISL and LF both were stiffer than were the human ligaments.

The completely assembled FE model (intact configuration) was compared with bilateral hemifacetectomy, complete facetectomy, and human lumbar segment (L4–L5)[20] configurations. The total RoM in flexion and extension under a 10-Nm moment of bending is shown in Figure 5, during which the RoM in extension of the facetectomy configuration was increased (+48.4%) markedly compared with that of the intact configuration. The hemifacetectomy configuration showed intermediate RoM values during both flexion and extension. Qualitative individuation of the area relative to the position of the IAR is shown in Figure 6 for all the configurations relative to the porcine FE model. In the hemifacetectomy configuration, the putative IAR attachment site was situated at the posterior part of the caudal endplate, whereas the possible position of the IAR was concentrated more caudally for

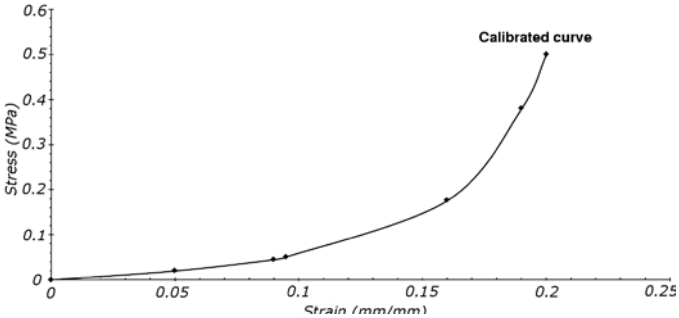

Figure 3. Calibrated stress–strain curve of the IVD defined in this study.

Table 2. Peak flexion–extension rotations predicted during the present porcine FE study for the various conditions of the calibration procedure

Condition	Peak flexion rotation (degrees)	Peak extension rotation (degrees)
No-FJ	7.7	9.1
No-LF	7.6	6.9
No-ISL	7.4	6.9
No-SSL	7.1	6.9
Intact	7.1	6.9

Predictions were based on data presented in reference 11.

the intact configuration than for hemifacetectomy. The IAR of the facetectomy configuration was near the center of the IVD.

Discussion

This study aimed to create and calibrate a detailed 3-dimensional FE model of the L4–L5 intact porcine segment by using an incremental calibration approach, based on data from in vitro testing of spinal specimens. We also investigated the influence of complete facetectomy and bilateral hemifacetectomy on the biomechanics of the L4–L5 intact porcine segment to reveal the configuration that most closely modeled human lumbar segment behavior. Accordingly, we developed the FE model and assessed the mechanical properties of its components. We then tested the model in flexion and extension and in various configurations including intact, hemifacetectomy, and complete facetectomy. We then compared the results with published data from a human intact lumbar segment (L4–L5).[20]

To perform the FE model calibration process, we incorporated in vitro RoM data obtained from a previously reported study.[11] To achieve high morphometric conformity, we acquired scanned computed tomography images pertaining to a single L4–L5 segment from a pig conforming to the characteristics assumed in the experimental study. Subsequently, identical boundary conditions were assumed for the FE constructed model. The mechanical properties of the involved structures were then adapted in order to generate totally matching RoM outcomes.

The passive porcine spinal element contributions to in vitro flexion–extension have been defined by using a polynomial model:[7] the resistance offered by each of the spinal elements to the applied moment for a typical L4–L5 motion segment was estimated. Consequently, the results were represented as moment–angle curves, which were not transformable to the force–displacement curves achieved in this study to allow direct comparison. At the same time, published data concerning force–displacement curves for individual porcine spinal ligaments are unavailable. The force–displacement outcomes relative to the SSL, ISL, LF, and CL obtained in the present study appear reasonable in view of the validation process.

Previous FE studies concerning the human spine incorporated the IVD through various approaches: as an almost- incompressible solid [12] or fluid elements for the nucleus pulposus[26] and as a anisotropic solid, fiber-reinforced composite or a more complex continuum of elements for the annulus fibrosus.[25] Due to the paucity of experimental investigations concerning the mechanical properties of the different components of the porcine IVD, we modeled both the nucleus and annulus as an almost-incompressible unique material. The first approximated curve relied on published experimental stress–strain curves.[6] These experimental data regarded the stress–strain curves of the lumbar IVDs of minipigs as homogeneous materials, which seemed to be characterized by increased stiffness as compared with the final calibrated curve obtained in the present study. This incongruity may reflect the marked differences between the specimens used in the studies,[6,11] in that 1 study[6] reports stress–strain material properties for porcine lumbar IVD loaded in compression, whereas the other[11] addressed IVD properties during flexion–extension bending. Regardless, we consider that the stress-strain curve achieved in the present study can be considered practical for the specimen we used, in the absence of more detailed experiments that might provide insight into the specific characteristics of the IVD components.

Data regarding the mechanical properties of the cancellous and cortical bone of the porcine vertebral body were obtained from published studies;[15,21] in contrast, we assumed that the Young modulus and Poisson ratio of posterior bone were similar to those of human lumbar spine.[4,10] However, we believe that the biomechanical behavior of the model was not altered markedly because the applied moments were unlikely to deform the bone due to its high stiffness values with respect to the ligaments and IVD.

The calibrated mathematical model of the porcine lumbar segment can simulate the behavior of the spine in situations in which other means of investigation are not feasible: the equivalent in vivo investigations on animals are difficult to manage logistically. In vitro experiments using animal cadavers are free from these restrictions, but they provide limited information and cannot simulate the muscle structures or neuromuscular controls present in vivo. Conversely, mathematical modeling yields information that laboratory experiments cannot provide, such as the effects of stresses in the disc and vertebrae. Such modeling also allows exploration of an essentially limitless range of physiologic conditions and combinations of conditions. Similarly, FE analysis permits exploration of a vast range of different treatment options and surgical interventions and allows 'testing' and optimization of prostheses even before their manufacture.[9] Mathematical models can become powerful tools to advance understanding, prevention, and treatment of spinal disorders. However, the results of mathematical models must be interpreted carefully from an appropriate biologic and clinical perspective before the results are applied to patients. In addition, more computed tomography images from more animals are needed to validate available data and to reveal any breed-specific differences in sizes and length of the lumbar segment.

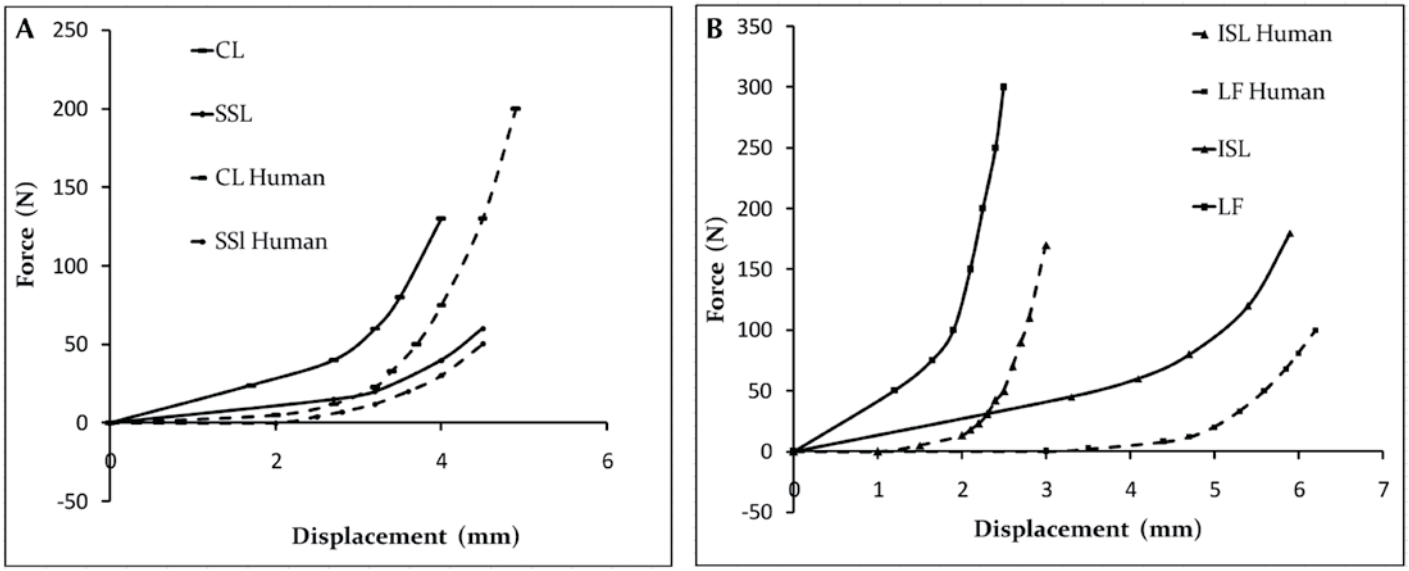

Figure 4. Force–displacement curves for the ligaments of the calibrated porcine FE model defined in this study compared with those from a study on the human spinal ligaments.[20](A) CL and SSL human ligaments compared to the respective porcine ligaments. (B) ISL and LF human ligaments compared to the respective porcine ligaments.

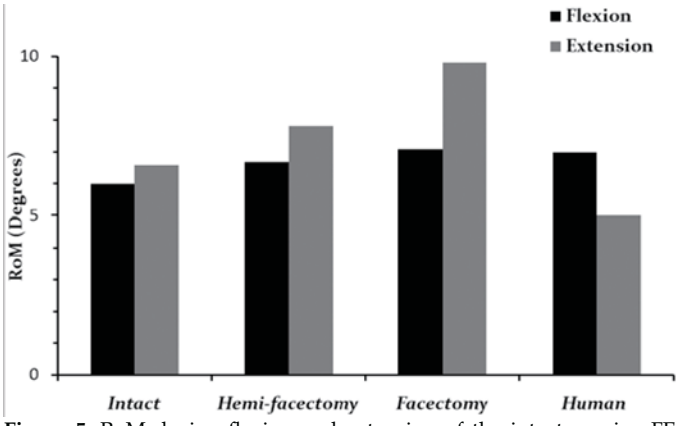

Figure 5. RoM during flexion and extension of the intact porcine FE model in comparison with those of the hemifacetectomy configuration, complete facetectomy configuration, and corresponding human lumbar FE model.[20]

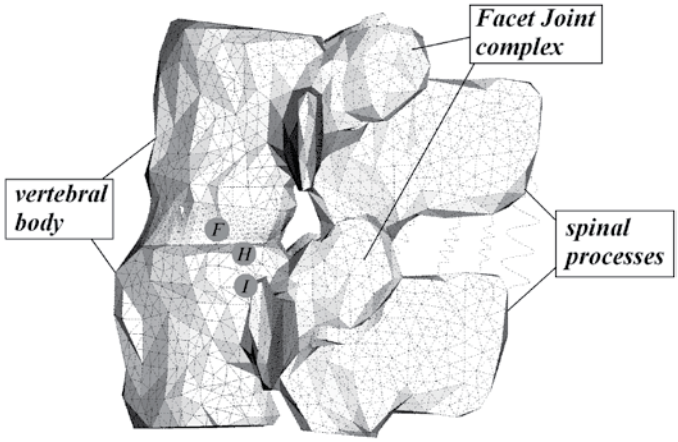

Figure 6. Qualitative representation of the area to which the IAR shifts during extension of the intact (I), the hemifacetectomy (H), and the complete facetectomy (F) configurations.

The numeric results obtained in the current study for the 3 porcine lumbar configurations (intact, hemifacetectomy, and complete facetectomy), especially regarding RoM, were low in terms of the angle achieved at the peak flexion moment compared with the peak extension moment. This unexpected difference may be associated with the actual neutral position of the segment. In fact, the exact location of the neutral position during the transition between flexion and extension in the in vitro tests[11] was not specifically defined by the authors. When assuming the neutral position in the middle of the experimental laxity zone, the RoM of the extension increase and the RoM of flexion decrease.

Our results reveal marked increases in extension RoM with respect to the complete facetectomy configuration. This increase was reasonable given that the FJ complex was the only structure contributing in extension during both the in vitro and computational tests. Importantly, in our results, the RoMs of the intact and hemifacetectomy configurations were highly comparable to that for the human segment.

Several experiments regarding the human IAR position in extension[23] estimated the possible location of the IAR to the posterior part of the lower endplate. The current study showed that in the porcine lumbar spine, this position could be gained only through bilateral hemifacetectomy. In addition, the bilateral hemifacetectomy configuration of the porcine segment was qualitatively equivalent to human morphometry because of dissection of the posterior closing of the porcine FJ. In fact, even if the RoM of the porcine intact configuration equivalent to that of the human segment, caudal displacement of the IAR might indicate posterior translation of the IVD. This aspect could be important to consider when choosing the appropriate animal model of spinal conditions, especially when evaluating models for spinal stabilization through interspinous posterior instrumentation.

Experimental validation of the bilateral hemifacetectomy configuration of the porcine lumbar segment is needed. The hemifacetectomy computational cut plane was oriented in order to disconnect the posterior closing contribution of the FJ contour, which is easily replicated experimentally. Therefore, our findings may provide the foundation for experimental studies aiming to identify an animal model that effectively describes the biomechanics of passive elements of the human lumbar spine.

References

1. **Akahoshi S, Sakai A, Arita S, Ikeda S, Morishita Y, Tsutsumi H, Ito M, Shiraishi A, Nakamura T.** 2005. Modulation of bone turnover by alfacalcidol and/or alendronate does not prevent glucocoticoid-induced osteoporosis in growing minipigs. J Bone Miner Metab **23:**341–350.
2. **An HS, Lim TH, You JW, Hong JH, Eck J, McGrady L.** 1995. Biomechanical evaluation of anterior thoracolumbar spinal instrumentation. Spine **20:**1979–1983.
3. **An YH, Friedman RJ.** 1999. Animal models in orthopedic research. Boca Raton (FL): CRC Press. p 505–566.
4. **Bellini CM, Galbusera F, Raimondi MT, Mineo GV, Brayda-Bruno M.** Biomechanics of the lumbar spine after dynamic stabilization. J Spinal Disord Tech. **20:**423–429.
5. **Brodke DS, Dick JC, Kunz DN, McCabe R, Zdeblick TA.** 1997. Posterior lumbar interbody fusion: a biomechanical comparison, including a new threaded cage. Spine **22:**26–31.
6. **Causa F, Manto L, Borzacchiello A, De Santis R, Netti PA, Ambrosio L, Nicolais L.** 2002. Spatial and structural dependence of mechanical properties of porcine intervertebral disc. J Mater Sci Mater Med **13:**1277–1280.
7. **Dickey JP, Gillespie KA.** 2003. Representation of passive spinal element contributions to in vitro flexion-extension using a polynomial model: illustration using the porcine lumbar spine. J Biomech **36:**883–888.
8. **Dickey JP, Kerr DJ.** 2003. Effect of specimen length: are the mechanics of individual motion comparable in functional spinal units and multisegment specimens? Med Eng Phys **25:**221–227.
9. **Fagan MJ, Julian S, Mohsen AM.** 2002. Finite element analysis in spine research. Proc Inst Mech Eng (Part H) **216:**281–298.
10. **Fantigrossi A, Galbusera F, Raimondi MT, Sassi M, Fornari M.** 2007. Biomechanical analysis of cages for posterior lumbar interbody fusion. Med Eng Phys **29:**101–109.
11. **Gillespie KA, Dickey JP.** 2004. Biomechanical role of lumbar spine ligaments in flexion and extension: determination using a parallel linkage robot and a porcine model. Spine **29:**1208–1216.
12. **Goel VK, Clausen JD.** 1998. Prediction of load sharing among spinal components of a C5–C6 motion segment using the finite element approach. Spine **23:**684–691.
13. **Kato N, Koshino T, Saito T, Takeuchi R.** 1998. Estimation of Young's modulus in swine cortical bone using quantitative computed tomography. Bull Hosp Jt Dis **57:**183–186.
14. **Kirby MC, Sikoryn TA, Hukins DWL, Aspden RM.** 1989. Structure and mechanical properties of the longitudinal ligaments and ligamentum flavum of the spine. J Biomed Eng **11:**192–196.
15. **Lin RM, Tsai KH, Chang GL.** 1997. Distribution and regional strength of trabecular bone in porcine lumbar spine. Clin Biomech (Bristol, Avon) **12:**331–336.
16. **Long JH Jr, Pabst DA, Shepherd WR, McLellan WA.** 1997. Locomotor design of dolphin vertebral columns: bending mechanics and morphology of *Delphinus delphis*. J Exp Biol **200(Pt 1):**65–81.
17. **McLain RF, Yerby SA, Moseley TA.** 2002. Comparative morphometry of L4 vertebrae: comparison of large animal models for the human lumbar spine. Spine **27:**E200–E2006.
18. **O'Connell GD, Vresilovic EJ, Elliott DM.** 2007. Comparison of animals used in disc research to human disc geometry. Spine **32:**328–333.
19. **Oda I, Abumi K, Duosai L, Shono Y, Kaneda K.** 1996. Biomechanical role of the posterior elements, costovertebral joints, and rib cage in the stability of the thoracic spine. Spine **21:**1423–1429.
20. **Schmidt H, Heuer F, Drumm J, Klezel Z, Claes L, Wilke HJ.** 2007. Application of a calibration method provides more realistic results for a finite element model of a lumbar spinal segment. Clin Biomech (Bristol, Avon) **22:**377–384
21. **Teo JC, Si-Hoe KM, Keh JEL, Teoh SH.** 2006. Relationship between CT intensity, micro-architecture and mechanical properties of porcine vertebral cancellous bone. Clin Biomech (Bristol, Avon) **21:**235–244.
22. **Van Deursen DL, Snijders CJ, Kingma I, Van Dieen JH.** 2001. In vitro torsion-induced stress distribution changes in porcine intervertebral discs. Spine **26:**2582–2586.
23. **White A, Panjabi M.** 1990. Clinical biomechanics of the spine. Philadelphia: JB Lippincott.
24. **Wilke HJ, Kettler A, Claes LE.** 1997. Are sheep spines a valid biomechanical model for human spines? Spine **22:**2365–2374.
25. **Yin L, Elliott DM.** 2005. A homogenization model of the annulus fibrosus. J Biomech **38:**1674–1684.
26. **Yoganandan N, Kumaresan SC, Liming V, Pintar FA, Larson SJ.** 1996. Finite element modeling of the C4-C6 cervical spine unit. Med Eng Phys **18:**569–574.